LETTERS

Optical frequency comb generation from a monolithic microresonator

P. Del'Haye[1], A. Schliesser[1], O. Arcizet[1], T. Wilken[1], R. Holzwarth[1] & T. J. Kippenberg[1]

Optical frequency combs[1–3] provide equidistant frequency markers in the infrared, visible and ultraviolet[4,5], and can be used to link an unknown optical frequency to a radio or microwave frequency reference[6,7]. Since their inception, frequency combs have triggered substantial advances in optical frequency metrology and precision measurements[6,7] and in applications such as broadband laser-based gas sensing[8] and molecular fingerprinting[9]. Early work generated frequency combs by intra-cavity phase modulation[10,11]; subsequently, frequency combs have been generated using the comb-like mode structure of mode-locked lasers, whose repetition rate and carrier envelope phase can be stabilized[12]. Here we report a substantially different approach to comb generation, in which equally spaced frequency markers are produced by the interaction between a continuous-wave pump laser of a known frequency with the modes of a monolithic ultra-high-Q microresonator[13] via the Kerr nonlinearity[14,15]. The intrinsically broadband nature of parametric gain makes it possible to generate discrete comb modes over a 500-nm-wide span (~70 THz) around 1,550 nm without relying on any external spectral broadening. Optical-heterodyne-based measurements reveal that cascaded parametric interactions give rise to an optical frequency comb, overcoming passive cavity dispersion. The uniformity of the mode spacing has been verified to within a relative experimental precision of 7.3×10^{-18}. In contrast to femtosecond mode-locked lasers[16], this work represents a step towards a monolithic optical frequency comb generator, allowing considerable reduction in size, complexity and power consumption. Moreover, the approach can operate at previously unattainable repetition rates[17], exceeding 100 GHz, which are useful in applications where access to individual comb modes is required, such as optical waveform synthesis[18], high capacity telecommunications or astrophysical spectrometer calibration[19].

Optical microcavities[20] are, owing to their long temporal and small spatial light confinement, ideally suited for nonlinear frequency conversion, which has led to a marked reduction in the threshold of nonlinear optical processes[21–23]. In contrast to stimulated gain, parametric gain[24] does not involve coupling to a dissipative reservoir, is broadband as it does not rely on atomic or molecular resonances, and constitutes a phase-sensitive amplification process, making it uniquely suited for tunable frequency conversion. In the case of a material with inversion symmetry—such as silica—the nonlinear optical effects are dominated by the third-order nonlinearity. The parametric process is based on four-wave mixing (FWM) among two pump photons (frequency υ_P) with a signal (υ_S) and idler photon (υ_I) and results in the emergence of (phase-coherent) signal and idler sideband) at the expense of the pump. Observing parametric interactions requires both energy and momentum conservation to be satisfied. In a microcavity of the whispering gallery type[20] the optical modes are angular momentum eigenstates and have discrete propagation constants $\beta_m = m/R$ resulting from the periodic boundary condition, where the integer m denotes the angular mode number and R the cavity radius. Consequently, the conversion of two pump photons (propagation constant β_N) into adjacent signal and idler modes ($\beta_{N-\Delta N}$, $\beta_{N+\Delta N}$, $\Delta N = 1, 2, 3\ldots$) conserves momentum intrinsically[14]. On the other hand, energy conservation ($2h\upsilon_P = h\upsilon_I + h\upsilon_S$, where h is the Planck constant) places stringent conditions on cavity dispersion, because the frequency difference between adjacent modes $\upsilon_{FSR} = |\upsilon_m - \upsilon_{m+1}|$ (the free spectral range, FSR) can vary owing to both material and geometric dispersion, rendering the cavity modes non-equidistant. For modes sufficiently close to the pump, however, the accumulated variation in the FSRs can be small. Indeed under these circumstances, parametric frequency conversion has only recently been observed for the first time[14,15] in ultra-high-Q microcavities (made of crystalline[15] CaF_2 and silica[14,30]).

Importantly, this mechanism can also be used to generate optical frequency combs: the initially generated signal and idler sidebands can interact among each other and produce higher-order sidebands (Fig. 1) by non-degenerate FWM[26] which ensures that the frequency difference of pump and first-order sidebands $\Delta\upsilon \equiv |\upsilon_P - \upsilon_S| = |\upsilon_P - \upsilon_I|$ is exactly transferred to all higher-order sidebands. This can be readily seen by noting that, for example, the second-order sidebands are generated by mixing among the pump and first-order signal/idler sidebands (for example, $\upsilon_{S2} = \upsilon_P + \upsilon_S - \upsilon_I = \upsilon_P - 2\Delta\upsilon$), which rigidly determines the spacing of any successively higher sidebands (Fig. 1b). Thus, provided that the cavity shows low dispersion, the successive FWM to higher orders would intrinsically lead to the generation of phase-coherent sidebands with equal spacing, that is, an optical frequency comb. Note that the generation of an optical frequency comb in this fashion requires experimental verification, as the parametric process itself could in principle produce signal/idler sidebands that are only pair-wise equidistant (for example, through degenerate FWM to higher orders) but not mutually equidistant as required for comb generation. Here, we report that monolithic microresonators do indeed allow realization of massively cascaded sideband generation, whose perfect equidistance is confirmed to a level of 7.3×10^{-18} (when normalized to the optical carrier). We have thus demonstrated optical frequency comb generation from a continuously pumped microcavity.

We use ultra-high-Q monolithic microresonators in the form of silica toroidal microcavities[13] on a silicon chip, which possess long photon storage times (τ_0): that is, ultra-high quality factors ($Q = 2\pi\upsilon\tau_0 > 10^8$) and small mode volumes. Highly efficient coupling is achieved using tapered optical fibres[27]. Owing to the high circulating power, parametric interactions are readily observed at a threshold of about 50 μW. When pumping with a continuous-wave 1,550-nm laser source, we observe a massive cascade and multiplication of the parametric sidebands extending to both higher and lower

[1]Max Planck Institut für Quantenoptik (MPQ), Hans-Kopfermann-Strasse 1, 85748 Garching, Germany.

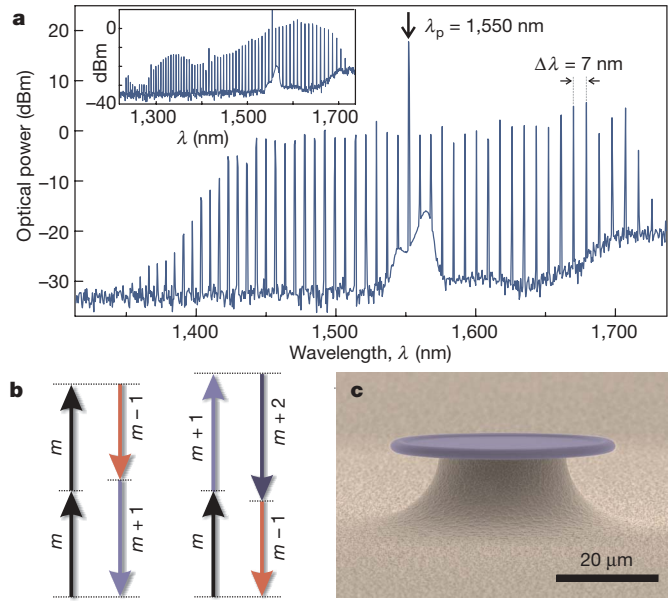

Figure 1 | Broadband parametric frequency conversion from a monolithic toroidal microresonator. **a**, Spectrum of the parametric frequency conversion observed in a 75-μm-diameter monolithic toroid microcavity when pumped with 60-mW continuous-wave laser power at 1,550 nm. The combination of parametric interactions and FWM gives rise to a broadband emission, spaced by the cavity free spectral range. Units of dBm represent logarithmic power relative to power of 1 mW. Inset: broadband parametric conversion of a different sample generating more than 70 parametric modes extending over a wavelength span of nearly 500 nm (pump power 130 mW). The asymmetry in the spectrum (with higher power in the higher-wavelength sidebands) is attributed to Raman amplification and variation of the tapered fibre output coupling. **b**, Schematic of the processes that contribute to the parametric conversion: degenerate (left) and non-degenerate (right) FWM among cavity eigenmodes. Momentum conservation is intrinsically satisfied for the designated angular mode number (m) combinations. **c**, Scanning electron microscope image of a toroid microcavity on a silicon chip.

frequencies. Figure 1a shows a spectrum in which a 75-μm-diameter microcavity was pumped with 60 mW power, giving rise to an intracavity intensity exceeding 1 GW cm^{-2}. The parametric frequency conversion could extend over more than 490 nm (see Fig. 1a inset), with the total conversion efficiency being 21.2%. These bright sidebands (termed Kerr combs in the remaining discussions) could be observed in many different samples, with conversion efficiencies of more than 83% by working in the over-coupled regime. In the largest fabricated samples (190 μm diameter), 380-nm broad Kerr combs comprising 134 modes spaced by 375 GHz could be generated at the expense of slightly higher pump power (see Supplementary Information).

To verify that the Kerr comb contains equidistant frequencies, we used a fibre-laser-based optical frequency comb[28] from Menlo Systems (termed reference comb in the remaining discussion) as a reference grid with a repetition rate of f_{rep} = 100 MHz. The principle underlying our measurement is that the beating generated on a photodiode by superimposing the reference comb with the Kerr comb will produce beat notes that constitute a replica of the optical spectrum in the radio frequency domain, similar to multi-heterodyne frequency comb spectroscopy[29] (see Supplementary Information). Specifically, if the Kerr comb is equidistant, the beat notes with the reference comb will constitute an equidistant comb in the radio frequency domain (with frequency spacing Δf, where $\Delta f = (\Delta \upsilon \bmod f_{rep})$). Figure 2a shows the experimental setup for the optical beat measurement. In brief, an external cavity laser operating at 1,550 nm was used to pump a microcavity. The generated Kerr modes were then superimposed with the reference comb in a beat note detection unit (BDU), consisting of polarizing optics for combining reference and Kerr comb and a grating to select the desired region of spectral overlap. In this manner, the beatings of nine simultaneously oscillating parametric modes (covering a wavelength span of more than 50 nm) were recorded, as shown in Fig. 2c. Remarkably, from the equidistant spacing of the radio frequencies, it is found that the generated sidebands are equidistant to within 5 kHz (as determined by the measurement time of 200 μs).

To improve the accuracy, we developed an additional experiment measuring the beat notes of three Kerr modes with the fibre-reference comb using three separate BDUs (Fig. 3a), each of which counted a single radio frequency beat (f_0, f_1, f_2). A signal-to-noise ratio exceeding 30 dB in a 500-kHz bandwidth was achieved, sufficient to use radio frequency counters, all referenced to a 10-MHz signal provided by a hydrogen maser. The beat note measured on BDU1 was used to

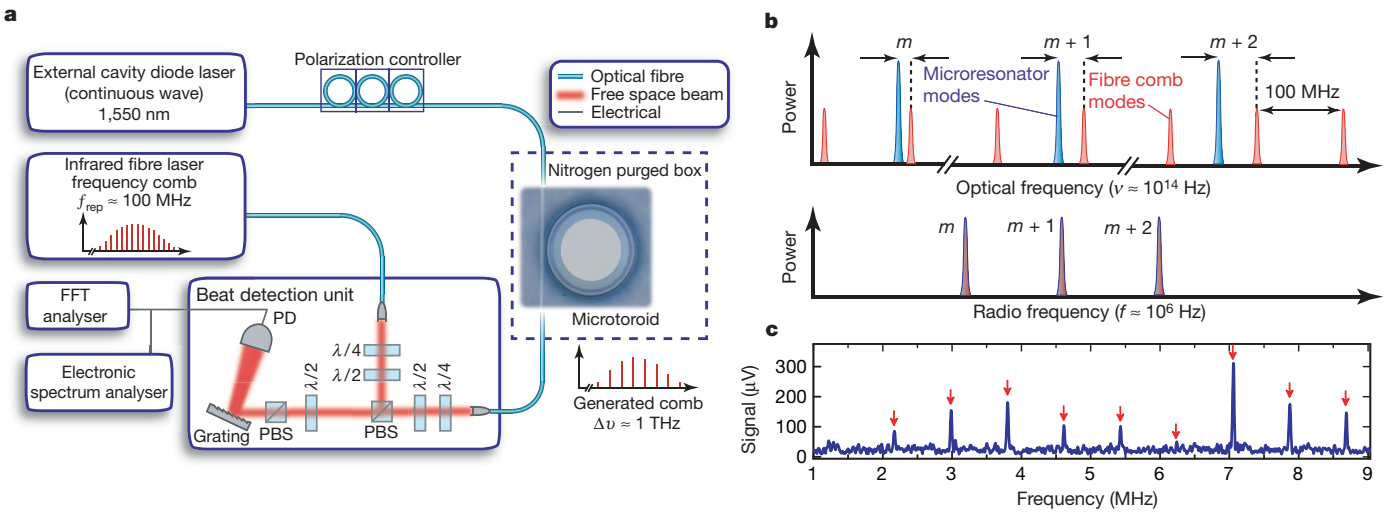

Figure 2 | Multi-heterodyne beat note detection. **a,** The experimental setup consisting of an external cavity laser (continuous wave) coupled to an ultra-high-Q monolithic microresonator in a nitrogen environment via a tapered fibre. The parametric output is coupled into one port of a BDU. The second port of the BDU is coupled to a mode-locked femtosecond erbium-doped fibre laser that serves as a reference comb. A grating is used to select a spectral region of the Kerr comb modes and a p-i-n silicon photodiode (PD) records their beatings with the reference comb (see Supplementary Information for details). PBS, polarizing beamsplitter; FFT, fast Fourier transform analyser. **b**, The measurement principle. The beating of the reference comb with the microcavity parametric modes yields beat frequencies in the radio frequency domain. **c**, Radio frequency spectrum of nine simultaneously oscillating Kerr modes, showing a uniform spacing.

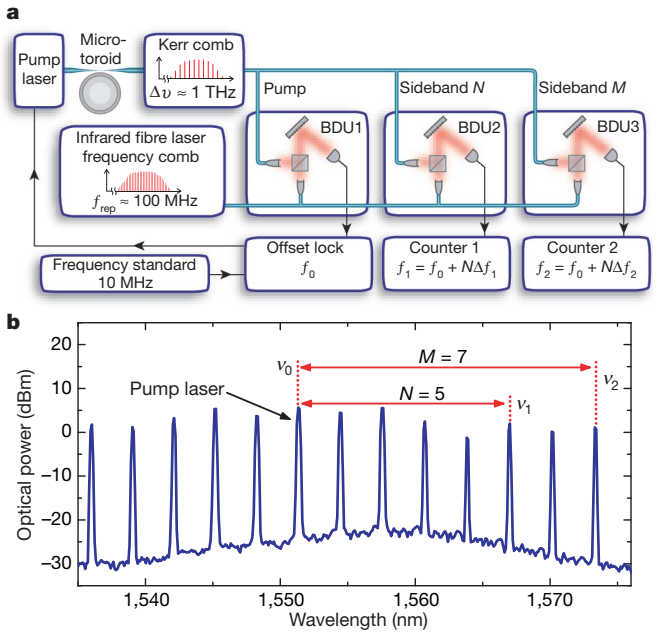

Figure 3 | Probing the equidistance of the comb structure. a, Simplified schematic of the setup which consists of three BDUs to measure the beating of three Kerr modes with the infrared fibre-based reference comb. All BDUs are referenced to the MPQ hydrogen maser as the frequency standard. The first BDU is used to produce a phase lock between one comb line of the reference comb and the pump laser (which constitutes one mode of the Kerr comb). **b**, The parametric spectrum used to validate the equidistance of the comb modes.

create an offset lock between a single reference comb mode and the pump laser by a known offset frequency (f_0). The second (third) counter measured the Nth (Mth) mode of the Kerr comb as shown in Fig. 3. For equidistant mode spacing, the second (third) BDU gives rise to the beat frequency $f_1 = f_0 + \Delta f \times N$ ($f_2 = f_0 + \Delta f \times M$). We then checked the uniformity of the Kerr comb by deriving the deviation from equidistant mode spacing, that is, $\varepsilon \equiv \frac{f_2 - f_1}{M - N} - \frac{f_1 - f_0}{N}$.

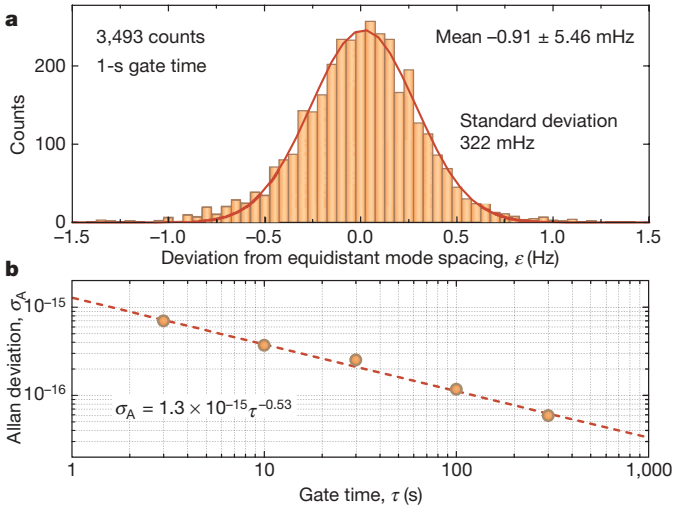

Figure 4 | Verification of the equidistant mode spacing. a, The deviation from equidistant mode spacing (ε) for a gate time of 1 s for the parametric spectrum and measurement setup described in Fig. 3. For this measurement 3,493 points were recorded. The solid red line is a gaussian fit to the distribution. The standard deviation of the mean implies an accuracy of the mode spacing at the millihertz level, confirming the comb-like structure of the parametric spectrum. **b**, Allan deviation as a function of gate time, showing an inverse square-root dependence, as determined by the fit (dashed red line).

Alternatively, the ratio $(f_1 - f_0)/(f_2 - f_0) = N/M$ was counted directly (using frequency mixing and ratio counting; see Supplementary Information). Figure 4a shows the measured gaussian distribution of ε for $N = 5$, $M = 7$ and a counter gate time τ of 1 s. The cavity modes of this measurement span 21 nm and yield a deviation from equidistance of $\varepsilon = (-0.9 \pm 5.5)$ mHz. The wavelength span covered by this measurement was limited by the gain bandwidth of an erbium doped fibre amplifier, which was necessary for amplification of the reference comb to ensure sufficient power to run three BDUs simultaneously at the required signal-to-noise ratio. The Allan deviation of ε, measured for several gate times, is reported in Fig. 4b. Table 1 shows the results for different gate times and for the two different counting methods (the complete list is contained in the Supplementary Information). The weighted average of these results verifies the uniformity of the comb spacing to a level of 7.3×10^{-18}, when referenced to the optical carrier. Normalized to the bandwidth of the measured Kerr lines (2.1 THz), this corresponds to 5.2×10^{-16}. This accuracy is on a par with measurements for fibre-based frequency combs[28] and confirms that the generated Kerr combs show uniform mode spacing.

Next we investigated the role of dispersion underlying the observed comb generation. Dispersion in whispering-gallery-mode microcavities is characterized by the variation in the FSR, $\Delta\upsilon_{FSR} = (\upsilon_{m+1} - \upsilon_m) - (\upsilon_m - \upsilon_{m-1}) = \upsilon_{m+1} + \upsilon_{m-1} - 2\upsilon_m$, and has two contributions. Geometrical cavity dispersion accounts for a negative FSR dispersion, given by $\Delta\upsilon_{FSR} \approx -0.41 \frac{c}{2\pi n R} m^{-\frac{5}{3}}$ where R is the cavity radius (see Supplementary Information). Material dispersion on the other hand is given by $\Delta\upsilon_{FSR} \approx \frac{1}{4\pi^2} \frac{c^2\lambda^2}{n^3 R^2} \cdot \mathrm{GVD}$, where $\mathrm{GVD} = -\frac{\lambda}{c} \frac{\partial^2 n}{\partial \lambda^2}$ is the group velocity dispersion parameter. Because the GVD of silica is positive for wavelength greater than 1.3 μm (anomalous dispersion), it can compensate[30] the intrinsic resonator dispersion (causing $\Delta\upsilon_{FSR} > 0$). Indeed we measured a positive dispersion (see Supplementary Information) which equates to only about 20 MHz over a span of about 60 nm. This low value indicates that the experiments are carried out close to the zero dispersion wavelength, in agreement with theoretical predictions.

Note that the residual cavity dispersion exceeding the 'cold' cavity linewidth does not preclude the parametric comb generation process. This could be explained in terms of a nonlinear optical mode pulling process as reported in ref. 14. The strong continuous-wave pump laser will induce both self-phase modulation and cross-phase modulation, the latter being twice as large as the former. The refractive index changes induced by self-phase and cross-phase modulation will shift the cavity resonance frequencies by different amounts, thereby causing a net change in the (driven) cavity dispersion from its passive (undriven) value[14]. This nonlinear mode pulling can provide a mechanism to compensate the residual cavity dispersion.

Regarding future applications in metrology, we note that absolute referencing can be attained by locking the pump laser frequency υ_0 to a known atomic transition and locking the mode spacing to a microwave reference (such as a caesium atomic clock). The latter requires the two degrees of freedom of the comb, its repetition rate (that is,

Table 1 | Experimental results on the deviation from equidistant mode spacing

Gate time (s)	Number of readings	Mean ε (mHz)	Standard deviation (mHz)	Relative accuracy	Counting method
1	3,493	-0.9 ± 5.5	322	2.7×10^{-17}	Two counters
3	173	5.8 ± 12.6	165	6.3×10^{-17}	Ratio counting
10	22	-17.9 ± 15.0	70	7.5×10^{-17}	Ratio counting
30	39	1.7 ± 7.4	46	3.7×10^{-17}	Ratio counting
100	42	-0.3 ± 2.7	17	1.4×10^{-17}	Ratio counting
300	14	-0.8 ± 2.8	11	1.4×10^{-17}	Ratio counting

The weighted mean of all measurements (including Supplementary Information) yields a relative accuracy of 7.3×10^{-18}.

mode spacing, $\Delta\upsilon$) and frequency offset (that is, $\upsilon_{CEO} = \upsilon_0 \bmod \Delta\upsilon$), to be controlled independently. We have already shown in a proof-of-concept experiment that it is possible to lock two modes of the Kerr comb simultaneously to two modes of the reference comb, showing that independent control of both υ_{CEO} and $\Delta\upsilon$ is possible. The two actuators used for this lock are the detuning of the pump laser from the microcavity resonance and the pump power, which affects the optical pathlength of the cavity via the thermal effect and the nonlinear phase shift.

A monolithic frequency comb generator could potentially prove useful for frequency metrology, given further improvements. Evidently a readily measurable repetition rate would be highly advantageous when directly referencing the optical field to a microwave signal[2]. To this end a 660-μm-diameter microcavity would already allow operating at repetition rates less than 100 GHz, which can be detected using fast photodiodes. On the other hand, a large mode spacing as demonstrated here could prove useful in applications such as line-by-line pulse shaping[18], calibration of astrophysical spectrometers[19] or direct comb spectroscopy. The high repetition rate from an on-chip device may also be useful in generating multiple channels for high capacity telecommunications (spacing 160 GHz) and low-noise microwave signals. Furthermore, we note that parametric interactions do also occur in other types of microcavities—for example, CaF_2 (ref. 15)—provided that the material shows a third-order nonlinearity and sufficiently long photon lifetimes. Therefore the cavity geometry is not conceptually central to the work and the reported phenomena should be observable in other types of high-Q microresonators, such as silicon, silicon-on-insulator or crystalline-based whispering-gallery-mode resonators. The recent observation of net parametric gain[25] on a silicon chip is a promising step in this direction.

Received 3 April; accepted 12 October 2007.

1. Udem, T., Holzwarth, R. & Hänsch, T. W. Optical frequency metrology. *Nature* **416,** 233–237 (2002).
2. Cundiff, S. T. & Ye, J. Colloquium: Femtosecond optical frequency combs. *Rev. Mod. Phys.* **75,** 325–342 (2003).
3. Ye, J. & Cundiff, S. T. *Femtosecond Optical Frequency Comb: Principle, Operation and Applications* (Springer, New York, 2005).
4. Jones, R. J., Moll, K. D., Thorpe, M. J. & Ye, J. Phase-coherent frequency combs in the vacuum ultraviolet via high-harmonic generation inside a femtosecond enhancement cavity. *Phys. Rev. Lett.* **94,** 193201 (2005).
5. Gohle, C. *et al.* A frequency comb in the extreme ultraviolet. *Nature* **436,** 234–237 (2005).
6. Diddams, S. A. *et al.* Direct link between microwave and optical frequencies with a 300 THz femtosecond laser comb. *Phys. Rev. Lett.* **84,** 5102–5105 (2000).
7. Reichert, J. *et al.* Phase coherent vacuum-ultraviolet to radio frequency comparison with a mode-locked laser. *Phys. Rev. Lett.* **84,** 3232–3235 (2000).
8. Thorpe, M. J., Moll, K. D., Jones, J. J., Safdi, B. & Ye, J. Broadband cavity ringdown spectroscopy for sensitive and rapid molecular detection. *Science* **311,** 1595–1599 (2006).
9. Diddams, S. A., Hollberg, L. & Mbele, V. Molecular fingerprinting with the resolved modes of a femtosecond laser frequency comb. *Nature* **445,** 627–630 (2007).
10. Kourogi, M., Nakagawa, K. & Ohtsu, M. Wide-span optical frequency comb generator for accurate optical frequency difference measurement. *IEEE J. Quantum Electron.* **29,** 2693–2701 (1993).
11. Ye, J., Ma, L. S., Daly, T. & Hall, J. L. Highly selective terahertz optical frequency comb generator. *Opt. Lett.* **22,** 301–303 (1997).
12. Jones, D. J. *et al.* Carrier-envelope phase control of femtosecond mode-locked lasers and direct optical frequency synthesis. *Science* **288,** 635–639 (2000).
13. Armani, D. K., Kippenberg, T. J., Spillane, S. M. & Vahala, K. J. Ultra-high-Q toroid microcavity on a chip. *Nature* **421,** 925–928 (2003).
14. Kippenberg, T. J., Spillane, S. M. & Vahala, K. J. Kerr-nonlinearity optical parametric oscillation in an ultrahigh-Q toroid microcavity. *Phys. Rev. Lett.* **93,** 083904 (2004).
15. Savchenkov, A. A. *et al.* Low threshold optical oscillations in a whispering gallery mode CaF_2 resonator. *Phys. Rev. Lett.* **93,** 243905 (2004).
16. Steinmeyer, G., Sutter, D. H., Gallmann, L., Matuschek, N. & Keller, U. Frontiers in ultrashort pulse generation: Pushing the limits in linear and nonlinear optics. *Science* **286,** 1507–1512 (1999).
17. Keller, U. Recent developments in compact ultrafast lasers. *Nature* **424,** 831–838 (2003).
18. Weiner, A. M. Femtosecond pulse shaping using spatial light modulators. *Rev. Sci. Instrum.* **71,** 1929–1960 (2000).
19. Murphy, M. T. *et al.* High-precision wavelength calibration with laser frequency combs. *Mon. Not. R. Astron. Soc.* **380,** 839–847 (2007).
20. Vahala, K. J. Optical microcavities. *Nature* **424,** 839–846 (2003).
21. Chang, R. K. & Campillo, A. J. *Optical Processes in Microcavities* (World Scientific, Singapore, 1996).
22. Spillane, S. M., Kippenberg, T. J. & Vahala, K. J. Ultralow-threshold Raman laser using a spherical dielectric microcavity. *Nature* **415,** 621–623 (2002).
23. Carmon, T. & Vahala, K. J. Visible continuous emission from a silica microphotonic device by the third harmonic generation. *Nature Phys.* **3,** 430–435 (2007).
24. Dunn, M. H. & Ebrahimzadeh, M. Parametric generation of tunable light from continuous-wave to femtosecond pulses. *Science* **286,** 1513–1517 (1999).
25. Foster, M. A. *et al.* Broad-band optical parametric gain on a silicon photonic chip. *Nature* **441,** 960–963 (2006).
26. Stolen, R. H. & Bjorkholm, J. E. Parametric amplification and frequency-conversion in optical fibers. *IEEE J. Quantum Electron.* **18,** 1062–1072 (1982).
27. Spillane, S. M., Kippenberg, T. J., Painter, O. J. & Vahala, K. J. Ideality in a fiber-taper-coupled microresonator system for application to cavity quantum electrodynamics. *Phys. Rev. Lett.* **91,** 043902 (2003).
28. Kubina, P. *et al.* Long term comparison of two fiber based frequency comb systems. *Opt. Expr.* **13,** 904–909 (2005).
29. Schliesser, A., Brehm, M., Keilmann, F. & van der Weide, D. W. Frequency-comb infrared spectrometer for rapid, remote chemical sensing. *Opt. Expr.* **13,** 9029–9038 (2005).
30. Agha, I. H., Okawachi, Y., Foster, M. A., Sharping, J. E. & Gaeta, A. L. Four-wave mixing parametric oscillations in dispersion-compensated high-Q silica microspheres. *Phys. Rev. A* **76,** 043837 (2007).

Supplementary Information is linked to the online version of the paper at www.nature.com/nature.

Acknowledgements We thank T. W. Hänsch, T. Udem, K. J. Vahala and S. A. Diddams for critical discussions and suggestions. T.J.K. acknowledges support via an Independent Max Planck Junior Research Group. This work was funded as part of a Marie Curie Excellence Grant (RG-UHQ), the DFG funded Nanosystems Initiative Munich (NIM) and a Marie Curie Reintegration Grant (JRG-UHQ). We thank J. Kotthaus for access to clean-room facilities for sample fabrication.

Author Information Reprints and permissions information is available at www.nature.com/reprints. Correspondence and requests for materials should be addressed to T.J.K. (tobias.kippenberg@mpq.mpg.de).